Metabolism and Anticancer Activity of the Curcumin Analogue, Dimethoxycurcumin

Constantin Tamvakopoulos,[1] Konstantinos Dimas,[1] Zacharias D. Sofianos,[1] Sophia Hatziantoniou,[2] Zhiyong Han,[3] Zhong-Li Liu,[4] James H. Wyche,[3] and Panayotis Pantazis[1,3]

Abstract

Purpose: The plant-derived compound curcumin has shown promising abilities as a cancer chemoprevention and chemotherapy agent *in vitro* and *in vivo* but exhibits poor bioavailability. Therefore, there is a need to investigate modified curcumin congeners for improved anticancer activity and pharmacokinetic properties.

Experimental Design: The synthetic curcumin analogue dimethoxycurcumin was compared with curcumin for ability to inhibit proliferation and apoptosis of human HCT116 colon cancer cells *in vitro* by estimating the GI_{50} and LC_{50} values and detecting the extent of apoptosis by flow cytometry analysis of the cell cycle. Metabolic stability and/or identification of metabolites were evaluated by recently developed mass spectrometric approaches after incubation with mouse and human liver microsomes and cancer cells *in vitro*. Additionally, circulating levels of dimethoxycurcumin and curcumin were determined in mice following i.p. administration.

Results: Dimethoxycurcumin is significantly more potent than curcumin in inhibiting proliferation and inducing apoptosis in HCT116 cells treated for 48 h. Nearly 100% of curcumin but <30% of dimethoxycurcumin was degraded in cells treated for 48 h, and incubation with liver microsomes confirmed the limited metabolism of dimethoxycurcumin. Both compounds were rapidly degraded *in vivo* but dimethoxycurcumin was more stable.

Conclusions: Compared with curcumin, dimethoxycurcumin is (*a*) more stable in cultured cells, (*b*) more potent in the ability to kill cancer cells by apoptosis, (*c*) less extensively metabolized in microsomal systems, and (*d*) more stable *in vivo*. It is likely that the differential extent of apoptosis induced by curcumin and dimethoxycurcumin *in vitro* is associated with the metabolite profiling and/or the extent of stability.

Curcumin (diferuloylmethane) is the active yellow pigment in turmeric, a popular plant-derived coloring spice and ingredient of many cosmetics and pharmaceuticals (see refs. 1–5 for reviews on structural and biological aspects of curcumin). In general, curcumin has been associated with a large number of biological and cellular activities/events, including antioxidative, anti-inflammatory, anticarcinogenic, and hypocholesterolemic properties (1–5), and a large number of studies have focused on the pathways by which curcumin acts as a chemoprotective agent (1, 2, 6, 7). Further, curcumin congeners have been reported to induce apoptosis, sensitize and overcome resistance to various agents that induce apoptosis in diverse human cancer cells (8–16), and decrease the occurrence of cardiomyocytic apoptosis after global cardiac ischemia/reperfusion (17). In general, curcumin mediates its effects by modulating several important molecular targets, including transcription factors, enzymes, cell cycle proteins, cytokines, receptors, and cell surface adhesion molecules (reviewed in refs. 2–4).

With regard to its anticancer potential, it has been shown that curcumin congeners can inhibit proliferation and/or induce apoptosis of cancer cells of diverse tissue origin, including B and T cells, colon, epidermis, prostate, breast, and head and neck squamous cell carcinoma, by arresting the cells in the G_2-M phase of the cell cycle; inhibiting transformation, tumor initiation, tumor invasion, angiogenesis, and metastasis; and inducing suppression of carcinogenesis of the skin, stomach, colon, and liver in mouse models (refs. 18, 19 and reviewed in refs. 3, 20, 21). In this context, curcumin induces apoptosis by a redox-dependent mechanism (18); reduction in the nuclear expression of nuclear factor-κB (19); inhibition of telomerase activity (22); down-regulation of Notch-1 signaling (23); and cytochrome *c* release, Bid cleavage and caspase-9 and caspase-3 activation, and down-regulation of the antiapoptotic proteins Bcl-2, Bcl-X_L, and Myc (20, 24). Further, depletion of endogenous glutathione sensitizes the cells to curcumin-induced apoptosis (24).

Authors' Affiliations: [1]Division of Pharmacology-Pharmacotechnology, Foundation for Biomedical Research, Academy of Athens; [2]School of Pharmacy, Department of Pharmaceutical Technology, University of Athens, Athens, Greece; [3]University of Oklahoma Cancer Institute, University of Oklahoma Health Sciences Center, Oklahoma City, Oklahoma; and [4]National Laboratory of Applied Organic Chemistry, Lanzhou University, Lanzhou, China

Received 7/26/06; revised 11/29/06; accepted 12/11/06.

The costs of publication of this article were defrayed in part by the payment of page charges. This article must therefore be hereby marked *advertisement* in accordance with 18 U.S.C. Section 1734 solely to indicate this fact.

Requests for reprints: Constantin Tamvakopoulos, Division of Pharmacology-Pharmacotechnology, Foundation for Biomedical Research, Academy of Athens, IIBEAA, 4 Soranou Efessiou Street, Athens 11527, Greece. Phone: 30-210-6597475; Fax: 30-210-6597510; E-mail: ctamvakop@bioacademy.gr.

doi:10.1158/1078-0432.CCR-06-1839

In phase I clinical trials, it was concluded that human volunteers tolerated a curcumin dose as high as 8 g/d with no side effects (25); however, these and other trials showed a very low systemic bioavailability in the plasma (reviewed in ref. 3). In view of serving as an agent for human cancer chemoprevention and therapy, curcumin bioavailability and metabolism have been studied in various systems. Curcumin shows poor systemic bioavailability in rodents and humans and undergoes extensive metabolic reduction and conjugation in the gastrointestinal tract (26–30).

In search of curcumin analogues with increased apoptotic efficacy against human cancer cells and/or less toxicity against physiologic (normal) cells and increased metabolic stability (bioavailability), we have investigated the compound dimethylcurcumin or dimethoxycurcumin, one of several synthetic curcumin congeners (31), which in preliminary studies showed exceptional antiproliferative activity against several human cancer cell lines. In this report, we show that dimethoxycurcumin is more potent than curcumin in the ability to induce apoptosis, at low concentrations, of HCT116 human colon cancer cells; is more stable than curcumin in treated HCT116 cells and human and mouse liver microsomes; and seems to have pharmacokinetic advantages in comparison with curcumin when given in mice. Finally, we report novel data on dimethoxycurcumin metabolic pathways.

Materials and Methods

Chemicals/biological reagents. Curcumin (>90% purity) was purchased from Extrasynthese (Genay Cedex, France). Dimethoxycurcumin was synthetically prepared as described (31) at the Department of Applied Chemistry, Lanzhou University (Lanzhou, China). Purity of dimethoxycurcumin was detected by high-performance liquid chromatography to be >90%. All solvents used in this study were liquid chromatography-mass spectrometry (LC-MS) grade. Acetonitrile, methanol, water, ammonium acetate, formic acid, and warfarin (Pestanal, analytic standard) were purchased from Fluka/Riedel-de Haën (St. Gallen, Switzerland). DMSO, trichloroacetic acid, sulforhodamine B, uridine 5′-diphosphoglucuronic acid, and β-NADPH were purchased from Sigma-Aldrich (St. Louis, MO). All cell culture reagents were purchased from Euroclone Life Sciences Division (Milan, Italy).

Cells, GI_{50}, and LC_{50}. Human colon carcinoma HCT116 cells were obtained from the National Cancer Institute (NIH, Bethesda, MD) and adapted to propagate in RPMI 1640 supplemented with 5% heat-inactivated FCS and antibiotics. Disposable plasticware for cell culturing and experimentation was obtained from Nunc (Roskilde, Denmark). The GI_{50} and LC_{50} values for curcumin and dimethoxycurcumin were estimated as described (32). HCT116 cells were seeded in 96-well plates at 5,000 in 0.5 mL medium per well, and then, the plates were incubated overnight at 37°C to allow the cells to adhere to the substrate and resume exponential proliferation. Subsequently, the medium and nonattached cells were aspirated and 0.2 mL of fresh medium was added, containing various curcumin and dimethoxycurcumin concentrations from 0.01 to 100 μmol/L. Stock curcumin and dimethoxycurcumin solutions were prepared in DMSO. The final DMSO concentrations in the cell cultures, ≤1% (v/v), have no effects on cell proliferation. Control cultures received DMSO alone. Four wells were used for each drug concentration. Incubation of untreated and drug-treated cells continued at 37°C for 48 h. At the end of the 48-h incubation period, the cells were fixed *in situ* with trichloroacetic acid followed by sulforhodamine B staining (33) and absorbance measurement at 530 nm on an EL-311 Biotek MicroELISA reader (BioTek Instruments, Winooski, VT). Each experiment was done three independent times and run in triplicates. GI_{50} (i.e., the drug concentration required to inhibit cell proliferation by 50%) and LC_{50} (i.e., the drug concentration required to kill 50% of the cultured cells) values were calculated as described (30) as the mean of the three

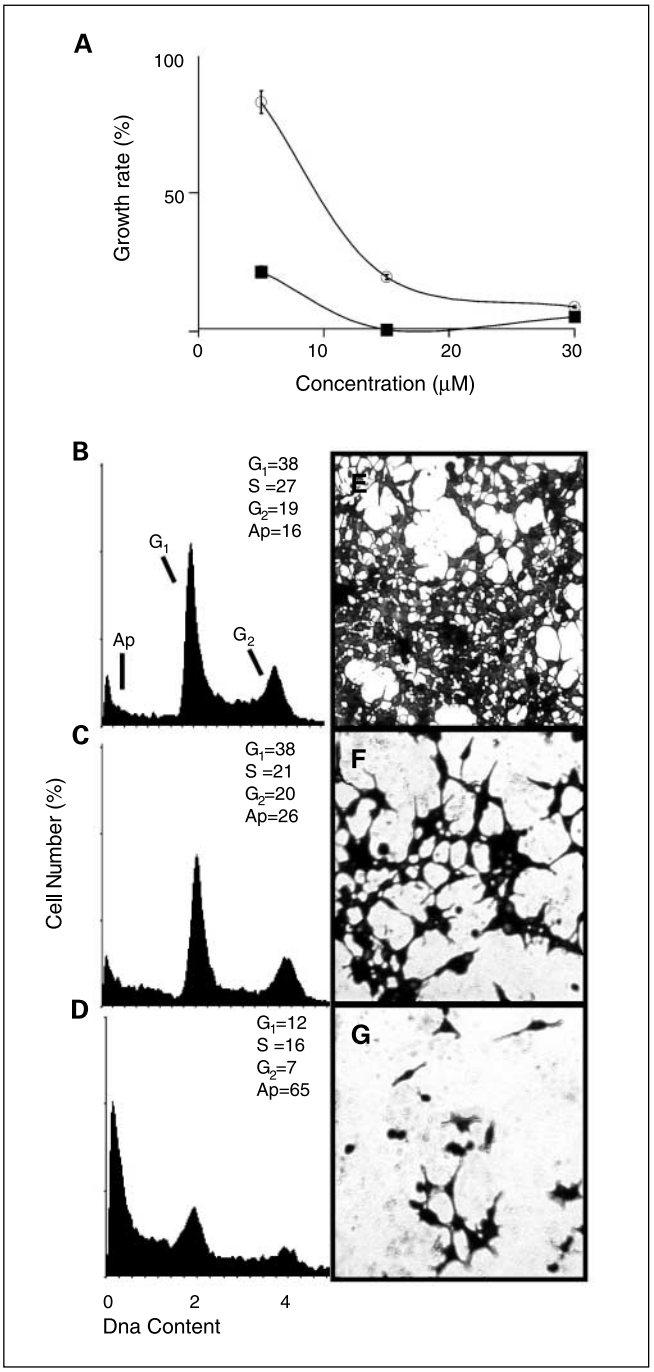

Fig. 1. Inhibition of proliferation and induction of apoptosis of cells treated with curcumin and dimethoxycurcumin. *A,* HCT116 cells were treated for 48 h with various concentrations of curcumin (○) and dimethoxycurcumin (■), and growth rates were estimated as percentage of growth of the untreated control cells. In another experiment, identical cell cultures were left untreated (*B* and *E*) or treated with 5 μmol/L of curcumin (*C* and *F*) or dimethoxycurcumin (*D* and *G*) for 48 h, and then, attached and detached cells were pooled and subjected to flow cytometry analysis of the cell cycle (*B-D*). *E* to *G,* in addition, the attached cells were photographed under a microscope. G_1, $G_0 + G_1$ cells; G_2, $G_2 + M$ cells; Ap, apoptotic cell fraction. Cell fraction calculations are shown as percentage of the total cell population. Results represent the mean of three independent experiments (coefficient of variation, <15%).

independent experiments. Once the GI_{50} and LC_{50} values were calculated, we selected to use those equimolar curcumin and dimethoxycurcumin concentrations, which showed the largest differences in the abilities to inhibit cell proliferation and induce apoptosis.

Flow cytometry and microscopy. Identical cultures of HCT116 cells were left untreated or treated with the desired drug concentrations for 48 h. Subsequently, untreated and drug-treated cells were subjected to flow cytometry analysis for detection of perturbations in the cell cycle and induction of apoptosis using an EPICS XL flow cytometer (Beckman Coulter, Miami, FL) and a MultiCycle AV program (Phoenix Flow Systems, San Diego, CA). The cell samples were treated with RNase and stained with propidium iodide immediately before analysis. Pools of both attached and detached cells were used in this analysis. We have used this methodology in several previous studies (34–37). Only attached cells, while in medium, were examined and photographed under phase-contrast microscopy.

Incubations with microsomes and cultured cells. Mouse liver microsomes (male CD-1) and human microsomes (CYPreme) were obtained from In Vitro Technologies (Leipzig, Germany). The metabolites of curcumin and dimethoxycurcumin were generated by incubation of curcumin and dimethoxycurcumin with microsomes in the presence of appropriate cofactors as described (26). Briefly, curcumin and dimethoxycurcumin (each at 10 μmol/L) were incubated for 1 h at 37°C with liver microsomes (1 mg protein; 20 mg/mL) and β-NADPH

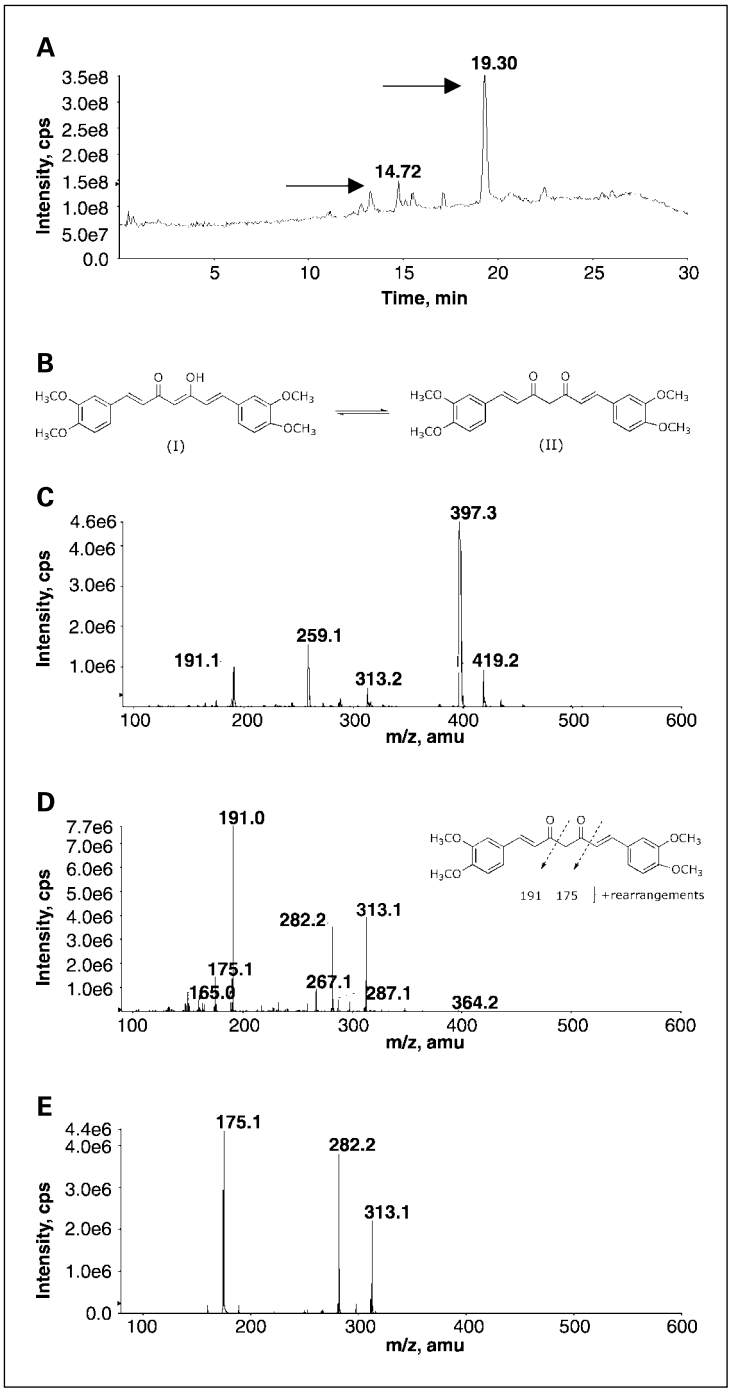

Fig. 2. Analyses of dimethoxycurcumin by MS methodologies. *A,* chromatogram of LC-MS analysis under gradient conditions. *B,* tautomeric forms of dimethoxycurcumin. I, enol; II, keto. *C,* full-scan spectrum of dimethoxycurcumin, $[M+H]^+$ shown at *m/z* 397. *D,* product ion spectra of ion *m/z* 397. *E,* MS/MS/MS fragmentation of first precursor ion, *m/z* 397, and second precursor ion, *m/z* 313.

Table 1. Dimethoxycurcumin metabolites

Dimethoxycurcumin metabolite (*m/z*)	Proposed transformation	Q1*	MRM† /EPI	Prec‡ /EPI
397	Parent compound	+	+	+
369	−28/2×(*O*-demethylation)		+	+
371§	−26/2×(*O*-demethylation)+H_2		+	+
383	−14/(*O*-demethylation)	+	+	+
385	−12/(*O*-demethylation)+H_2		+	+
399	+2/+H_2	+	+	+
401	+4/+2H_2		+	+
559	+162/(*O*-demethylation)+Glu		+	+
561	+164/(*O*-demethylation)+H_2+Glu		+	

*Detection by Q1 scan (*m/z* 90-800).
†Detection by MRM (based on transitions 397→191, 397→313, and known biotransformation reactions).
‡Precursor ion scan (of *m/z* 191).
§Observed in mouse microsome incubates only.

(1 mmol/L) in 50 mmol/L phosphate buffer solution (pH 7.2) in a final volume of 0.5 mL. To simulate phase II metabolism reactions, glucuronic acid (3 mmol/L) was included in the incubation mixture.

Cultures containing equal cell populations were treated with 15 μmol/L of curcumin or dimethoxycurcumin for various periods in 100-mm-diameter dishes. At selected times of treatment, the cell-conditioned medium was removed and saved, the attached cells were removed following mild trypsinization and collected in the saved cell-conditioned medium, and the suspension was gently centrifuged to pellet the cells. Subsequently, both cell pellets and clarified cell-conditioned medium were prepared for MS analysis of curcumin, dimethoxycurcumin, and their metabolites as described below.

Preparation of samples for LC-MS analysis. Following incubation of curcumin and dimethoxycurcumin with microsomes and cells, curcumin, dimethoxycurcumin, and their metabolites were extracted as follows: samples for LC-MS analysis were prepared by stepwise addition (0.5 mL followed by 1 mL) of acetonitrile to 0.5 mL suspension of microsomal or cell incubate and brief vortexing. The samples were then centrifuged for 5 min at 12,000 × *g*, and the supernatant (~1.2 mL) was transferred into glass tubes (12 × 75 mm) and evaporated in an SPD1010 SpeedVac system (ThermoSavant, Holbrook, NY) for 90 min at 55°C. An aliquot of 0.2 mL of mobile phase was added to each sample, vortexed, and then transferred to a 96-well plate for analysis.

In vivo *pharmacokinetic study.* For this study, we used 50 female *Rag1*^{tm1Mom} mice (The Jackson Laboratory, Bar Harbor, ME), 6 to 8 weeks old, weighing 22 to 24 g. Curcumin and dimethoxycurcumin were dissolved in DMSO and given i.p. at 2 μL/g of body weight (38) so that the final dose was 5 mg/kg of body weight. Approximately 500 μL of whole blood were collected after cardiac puncture in heparinized syringes at selected time points and transferred into microcentrifuge vials (Eppendorf) containing 10 μL heparin. Plasma was separated by centrifugation at 12,000 × *g* for 8 min and then stored at −80°C until extraction and LC-MS analysis as described below. Handling and experimentation of animals were according to Greek laws (2015/92), guidelines of the European Union and European Council (86/609 and ETS123, respectively), and Compliance with Standards for Human Care and Use of Laboratory Animals, NIH (Assurance No. A5736-0).

Metabolite identifications by LC-MS/MS. High-performance liquid chromatography was done with an Agilent 1100 Series System (Agilent Technologies, Waldbronn, Germany) equipped with a binary pump, autosampler, vacuum degasser, and temperature-controlled column compartment. The mobile phase consisted of solvents A (10% acetonitrile, 90% water, 2 mmol/L ammonium acetate, and 0.1% formic acid) and B (90% acetonitrile, 10% water, 2 mmol/L ammonium acetate, and 0.1% formic acid). A Waters Symmetry C8 column (3.5 μm, 2.1 × 50 mm; Waters Corp., Milford, MA) was used at a flow rate of 0.3 mL/min. Linear gradients (30 min) from 90% solvent A – 10% solvent B to 25% solvent A – 75% solvent B or from 80% solvent A – 20% solvent B to 20% solvent A – 80% B were used for separation of parent compound and metabolites. MS was done on a API 4000 QTRAP LC-MS/MS System fitted with a TurboIonSpray source and a hybrid triple-quadrupole/linear ion trap mass spectrometer (Applied Biosystems, Concord, Ontario, Canada). The instrument was operated in positive ion mode with a spray voltage of 5,500 V, a source temperature of 550°C, curtain gas (nitrogen) at 20, collision gas (nitrogen) at 5, ionsource gas 1 (air) at 40, and ionsource gas 2 (air) at 45 (arbitrary units). Data were acquired in various scan modes to provide quantification of curcumin or dimethoxycurcumin for the purpose of metabolite detection. Qualitative and structural information for curcumin and dimethoxycurcumin metabolites was obtained as follows: LC-MS/MS gradients were used to chromatographically separate curcumin and metabolites. Detection was achieved by Q1 or Q3 scan, enhanced MS, enhanced product ion (EPI), multiple reaction monitoring (MRM), neutral loss, precursor ion, and MS/MS/MS. The information-dependent acquisition feature of the instrument was used by combining either Q3 scan followed by EPI triggering or MRM followed by EPI triggering for targeted phase I and II analysis. The MRM transition lists created for this type of analysis (for curcumin or dimethoxycurcumin) were based on known biotransformation pathways (phase I and II metabolic reactions) stemming from transitions *m/z* 369.2→285.1, *m/z* 369.2→177.1 for curcumin and transitions *m/z* 397.2→313.1, *m/z* 397.2→191.1 for dimethoxycurcumin. Up to 65 MRM transitions were used per method with a dwell time of 40 ms. Information-dependent acquisition criteria were set so that several of the most intense MRM peaks (up to eight) would be selected for EPI analysis with a collision energy of 35 ± 5 V.

Quantification of curcumin and dimethoxycurcumin in mouse plasma. Stock solutions of both curcumin, dimethoxycurcumin (5-5,000 ng/mL) and warfarin (50 ng/mL), which was used as internal standard, were prepared in 50% acetonitrile in water containing 0.1% formic acid. A set of solutions at two different concentrations (100 and 2,500 ng/mL) was prepared to be used for quality control samples. Calibration curves (1-1,000 ng/mL) and quality control samples (20 and 500 ng/mL) were prepared by adding 50 μL of plasma (female CD-1 mouse) to 10 μL of the curcumin or dimethoxycurcumin solutions and 20 μL of internal standard. For the analysis of samples from the *in vivo* assay, 50 μL of plasma were added to 20 μL of internal standard. Protein precipitation was achieved by stepwise addition (2 × 150 μL) of acetonitrile and brief vortexing. The samples were then centrifuged for 5 min, and the supernatant was transferred into glass tubes and evaporated in an SPD1010 SpeedVac for 75 min at 50°C. An aliquot of 200 μL of mobile phase was added to each sample, vortexed, and then transferred to a 96-well plate for analysis. The high-performance liquid chromatography system described above was used

with a mobile phase that consisted of solvents A (10% acetonitrile, 90% water, 2 mmol/L ammonium acetate, and 0.1% formic acid) and B (90% acetonitrile, 10% water, 2 mmol/L ammonium acetate, and 0.1% formic acid). A Waters Symmetry C8 column (3.5 μm, 2.1 × 50 mm) was used at a flow rate of 0.3 mL/min. A linear gradient (11.5 min) from 65% solvent A – 35% solvent B to 35% solvent A – 65% solvent B was used for separation of curcumin and internal standard. Dimethoxycurcumin was separated from the internal standard under isocratic conditions (55% solvent A – 45% solvent B). Quantification for curcumin, dimethoxycurcumin, and internal standard was achieved in the MRM-positive mode. The transitions *m/z* 369.2→285.1 and *m/z* 397.2→313.1 were optimized by adjustments of collision energy, declustering potential, and dwell time for the analysis of curcumin and dimethoxycurcumin, respectively. Internal standard was monitored using the MRM transition *m/z* 309.1→162.9. Other MS conditions used for this experiment (e.g., TurboIonSpray source settings) are described above.

Results

***Cytotoxicity* in vitro.** The GI_{50} and LC_{50} values for curcumin and dimethoxycurcumin were estimated according to a published colorimetric cytotoxicity assay for anticancer drug screening (30). For curcumin, the GI_{50} and LC_{50} were calculated to be 10.2 and 109.2 μmol/L, respectively, whereas for dimethoxycurcumin the GI_{50} and LC_{50} were 3.3 and 38.2 μmol/L, respectively. Variations in GI_{50} and LC_{50} values, in replicate experiments, were <5%. These GI_{50} and LC_{50} values were observed after the compounds were incubated with HCT116 cells for 48 h. On consideration of the GI_{50} and LC_{50}, we investigated the percentage of growth inhibition in identical cell cultures treated with 5 to 50 μmol/L of curcumin and dimethoxycurcumin. The results (Fig. 1A) indicated that 5 μmol/L of curcumin and dimethoxycurcumin inhibited cell proliferation by approximately 20% and 80%, respectively; that is, dimethoxycurcumin was dramatically more effective than curcumin. At a 15 μmol/L concentration, curcumin inhibited cell proliferation by ~80%, whereas dimethoxycurcumin resulted in virtually complete inhibition of proliferation. Further, concentrations of 30 and 50 μmol/L were both highly antiproliferative (toxic), and therefore, no differences could be observed in the effectiveness of curcumin and dimethoxycurcumin at these concentrations.

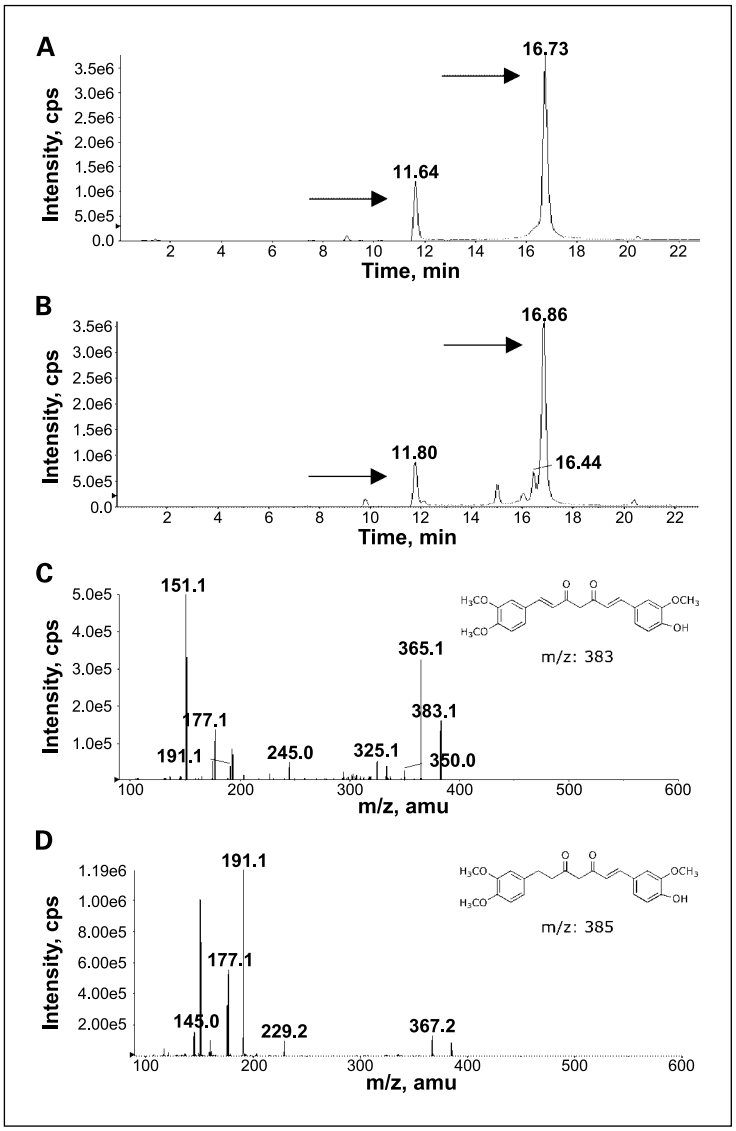

Fig. 3. Dimethoxycurcumin metabolites in microsomal preparations. *A,* dimethoxycurcumin in the absence of microsomes (control). *B,* dimethoxycurcumin in the presence of microsomes. *C,* spectrum of *O*-demethylated dimethoxycurcumin. *D,* spectrum of *O*-demethylated dihydrodimethoxycurcumin.

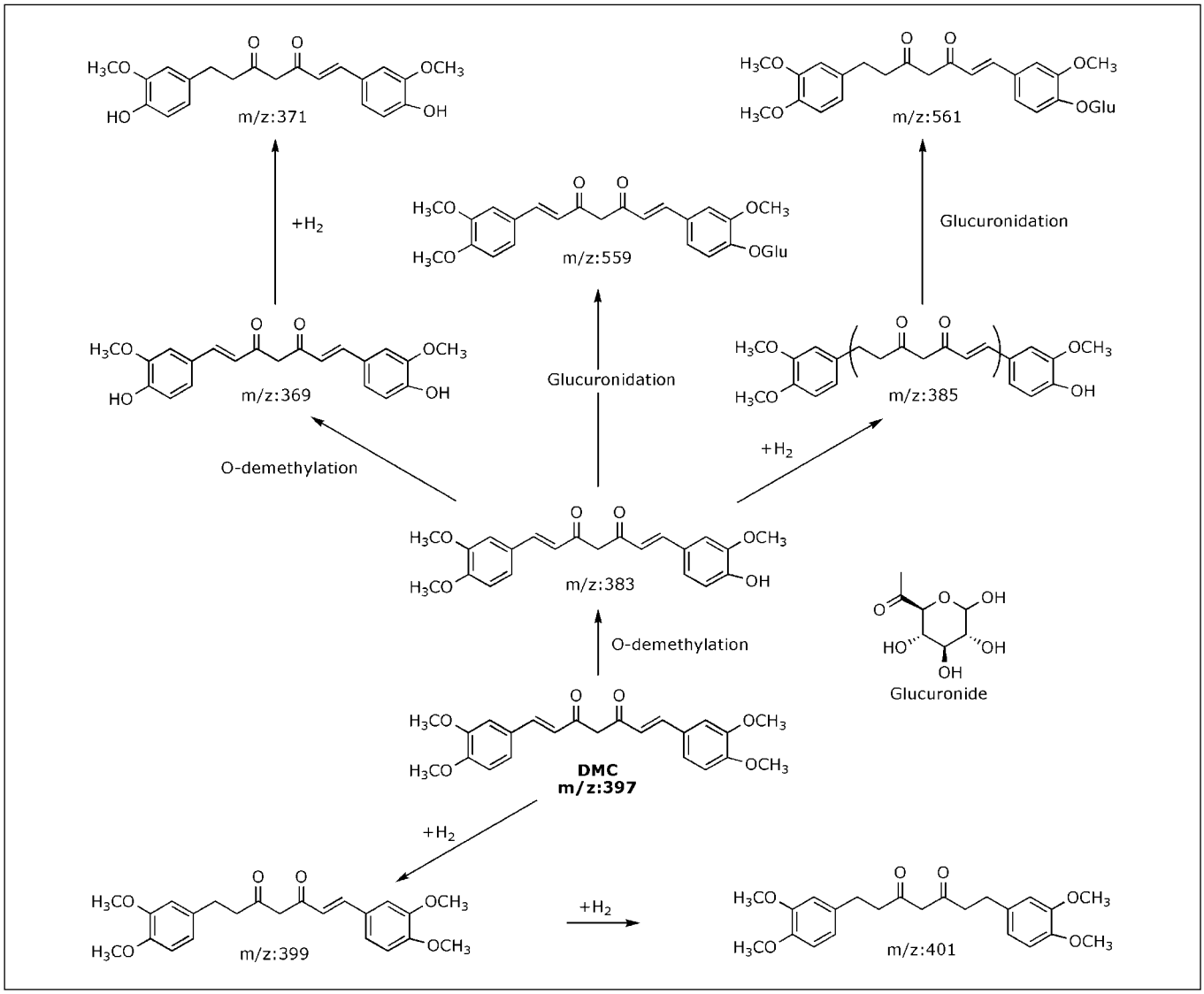

Fig. 4. Proposed scheme of dimethoxycurcumin (*DMC*) metabolic pathway.

Flow cytometry analysis of apoptosis and microscopy. The findings on the differential effectiveness of equal curcumin and dimethoxycurcumin concentrations on cell proliferation (see Fig. 1A) prompted us to use concentrations under 10 μmol/L in flow cytometry studies to be able to monitor changes in the cell cycle. Identical cell cultures were treated with 5 μmol/L of curcumin or dimethoxycurcumin for 48 h, and attached plus nonattached/detached cells were pooled and subjected to analysis of relative DNA content to detect cell cycle perturbations and apoptotic cell populations. After seeding the cells and an overnight adaptation period at 37°C, the medium containing nonattached cells was not replaced with fresh medium, and therefore, the apoptotic fraction of ~16% estimated was rather due to the presence of nonattached cells that eventually died in the untreated culture (Fig. 1B). Treatment of the cells with curcumin resulted in an increase in the apoptotic fraction (Fig. 1C), considering that apoptotic cells (16%) were already present in the control culture. However, dimethoxycurcumin treatment resulted in a large apoptotic fraction in the culture, accounting for ~65% of the total cell population (Fig. 1D). This dramatic increase in the apoptotic fraction, after dimethoxycurcumin treatment, resulted in concomitant decreases in G_1, S, and G_2 fractions, but this experiment would not indicate whether the cells entered apoptosis at a particular phase of the cell cycle. Also in the same study, we observed the density of the attached cells under the same magnification of a microscope (Fig. 1E-G). Forty-eight hours after adding curcumin and dimethoxycurcumin to the cultures, the cell density in the curcumin-treated culture was lower than that in the untreated control culture (compare Fig. 1E with Fig. 1F). Further, the effect of equal dimethoxycurcumin concentration (Fig. 1G) was more dramatic than that of curcumin on the cell density. Moreover, no attached cells were present in the cultures treated with 30 μmol/L of curcumin or dimethoxycurcumin (photos not shown). These results of the microscopy study confirmed the proliferation rate measurements (Fig. 1A) and the flow cytometry study results that dimethoxycurcumin is more efficient than an equal concentration of curcumin at a relatively low range of concentrations.

Fragmentation patterns. Figure 2A depicts a chromatogram of dimethoxycurcumin subjected to gradient conditions as described in Materials and Methods. As with curcumin, the keto-enol tautomerism at low pH conditions favors the keto form (Fig. 2B, *II*; refs. 39, 40), with a retention time of ~19.3 min, in comparison with the enol form (Fig. 2B, *I*), with a retention time of ~14.7 min (Fig. 2B). Figure 2C depicts a full spectrum of dimethoxycurcumin in Q1 scan mode. A major ion representing the $[M+H]^+$ ion, characteristic of dimethoxycurcumin, was observed at *m/z* 397. Other ions on the same spectrum represent sodium adducts at *m/z* 419 and in source fragmentation ions at *m/z* 191, 259, and 313. The molecular ion, *m/z* 397, shown in Fig. 2C, can be further fragmented in MS/MS mode to yield a spectrum (Fig. 2D) characteristic of dimethoxycurcumin. Tentative assignments for the major ions formed (e.g., *m/z* 191) are shown in Fig. 2D (*inset*). Such assignments are based on comparisons with MS/MS spectra of the structural analogue of dimethoxycurcumin, curcumin, and previously reported results on the mass fragmentation pattern of curcumin (41, 42). It is possible to select ions shown in Fig. 2D and do MS/MS/MS experiments. An example is shown in Fig. 2E, where the spectrum has been generated by selecting the first precursor ion, *m/z* 397, and the second precursor ion, *m/z* 313.

Identification of metabolites. Dimethoxycurcumin was incubated with mouse liver microsomes in the presence of glucuronic acid. Parent compound and metabolites were extracted and analyzed by LC-MS/MS. Detection and identification of metabolites were based on several experimental designs that are summarized in Table 1. LC followed by Q1 scan mode is a good approach that mainly allows detection of the most abundant metabolites because scanning in full mass range (*m/z* 90-800) does not allow the identification of metabolites in complex biological samples (e.g., microsomes) that are present at low concentrations. The design of experiments in which the precursor ion scan mode was combined with EPI was based on our knowledge that dimethoxycurcumin in MS/MS mode would yield characteristic ions, such as *m/z* 191 (see Fig. 2D). The assumption that metabolites of dimethoxycurcumin (analogues of the parent compound) would yield ions at *m/z* 191 under MS/MS conditions followed by information obtained from EPI allowed us to detect metabolites that were not identified by conventional LC-MS approaches (e.g., LC followed by Q1 scan). In a different experimental design of information-dependent acquisition experiments, 55 MRM transitions that corresponded to possible metabolites of dimethoxycurcumin were monitored. Such MRM transitions were used as survey scans, and following peak detection (when a certain threshold was reached), an EPI spectrum was generated to provide structural information for metabolite assignments. Similar approaches for metabolite detection using a hybrid triple-quadrupole linear ion trap instrument have been described (43, 44). A comparison between MRM chromatograms of dimethoxycurcumin incubated in the presence and absence of microsomes for 1 h is shown in Fig. 3A and B, respectively. A slightly faster gradient was used for separation of dimethoxycurcumin and metabolites that resulted in the elution of the two dimethoxycurcumin peaks in approximately 11.6 and 16.7 min (Fig. 3A, *arrows*). Metabolism of dimethoxycurcumin was significantly less extensive in comparison with curcumin (data not shown), with most of dimethoxycurcumin remaining intact following incubation with microsomes (Fig. 3B, *arrows*). Major metabolites were characterized by EPI, and examples of identified metabolites and MS/MS spectra are shown in chromatograms Fig. 3C and D for *O*-demethylated dimethoxycurcumin and *O*-demethylated dihydrodimethoxycurcumin, respectively. The metabolites of dimethoxycurcumin identified by the described approach are summarized in Table 1. The various scan modes, Q1, neutral loss, precursor ion, and MRM followed by EPI, represent a rather exhaustive analysis and characterization of metabolites. In addition, whenever metabolites of known structure were detected (e.g., curcumin), their MS/MS spectra were compared with previously reported studies (41). In general, the metabolism of dimethoxycurcumin was similar in human and mouse liver microsomes. Major metabolic pathways for dimethoxycurcumin were *O*-demethylation followed by formation of dihydroderivatives. Based on the data we obtained, we propose scheme I (Fig. 4) to illustrate the tentative dimethoxycurcumin pathway of metabolites. Major proposed metabolites were *O*-demethyl dimethoxycurcumin, dihydrodimethoxycurcumin, tetrahydrodimethoxycurcumin, and dihydro *O*-demethyl dimethoxycurcumin. It should be noted that the site of hydration for dihydro *O*-demethyl dimethoxycurcumin, as drawn in Fig. 4 (*m/z* 385), is tentative because it would also be possible to have hydration at the site proximal to the phenyl ring with the hydroxyl group. Further analysis and spectroscopic approaches

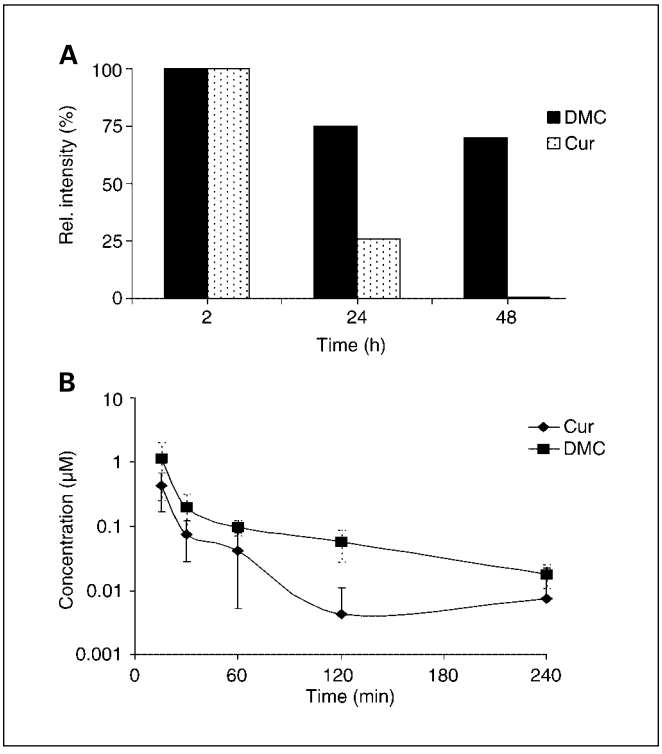

Fig. 5. Curcumin (*Cur*) and dimethoxycurcumin stability detected by LC-MS/MS. *A,* stability in cultured cells. Curcumin and dimethoxycurcumin were added to cultures of HCT116 cells, and their presence in cells was relatively quantified at 2, 24, and 48 h. The concentration at 2 h was taken as 100% of peak height. *B,* stability in mouse. Curcumin and dimethoxycurcumin were injected i.p. in mice ($n = 6$, $n = 4$ for each time point for curcumin and dimethoxycurcumin, respectively) at 5 mg/kg of body weight, and compound concentrations (μmol/L) were detected in plasma samples collected at 15, 30, 60, and 120 min.

(e.g., nuclear magnetic resonance) would be necessary for unequivocal structure assignments.

Stability of compounds in cultured cells. To compare the stability of curcumin and dimethoxycurcumin in cultured cells, curcumin and dimethoxycurcumin were added to identical cultures of HCT116 cells and incubated for 2, 24, and 48 h at 37°C. At the end of each incubation period, curcumin and dimethoxycurcumin were extracted from the cells by protein precipitation and subsequently analyzed by LC-MS/MS for relative quantification. For this experiment, the peak height of each compound at 2 h was taken as 100% (Fig. 5A). At 24 h, the dimethoxycurcumin and curcumin heights detected from the cells had decreased to 75% and 25%, respectively, whereas at 48 h the corresponding heights were at 70% and ~0% for dimethoxycurcumin and curcumin (Fig. 5A). These findings collectively showed that, unlike curcumin, dimethoxycurcumin was stable in human colon cancer cells.

In vivo *administration of curcumin and dimethoxycurcumin.* To compare the stability of curcumin and dimethoxycurcumin in mice, both compounds were given i.p. A low dose of 5 mg/kg in DMSO was chosen for this preliminary assessment to ensure solubility of both compounds. Although clearance for both compounds was rapid from the plasma, dimethoxycurcumin had overall higher mean levels in comparison with curcumin for all time points tested (~3-fold). Particularly at later time points (120 and 240 min), curcumin plasma concentrations were below the limit of quantification (~3 nmol/L) for most animals tested, whereas following dimethoxycurcumin dosing plasma concentrations were detectable for all time points. Concentrations of curcumin and dimethoxycurcumin as a function of time following administration in mice are depicted in Fig. 5B. Although this particular administration route (i.p.) yielded high variability with respect to concentrations at each time point, mean differences between the two compounds indicate that dimethoxycurcumin is more stable *in vivo* in comparison with curcumin.

Discussion

The plant-derived compound curcumin has been extensively studied as a chemopreventive agent (1, 6, 7) and, more recently, for its antineoplastic effects or as an adjunct in overall cancer treatment (8–15). In this regard, comparative studies have shown that the synthetic compound dimethoxycurcumin is more potent than its congener, curcumin, in the ability to serve as androgen receptor antagonist in human prostate cancer cells *in vitro* (45).

In this report, we have described experimental findings to show that dimethoxycurcumin is more effective than curcumin in inhibiting cell proliferation and inducing apoptosis *in vitro*. Specifically, dimethoxycurcumin is about two to four times more potent than curcumin when both compounds are compared at concentrations of 5 to 15 μmol/L. This was concluded on treating human colon cancer HCT116 cells with both compounds for 48 h and (*a*) measuring the GI_{50} and LC_{50} values by a standard colorimetric assay, (*b*) calculating the percentage of inhibition of the proliferation rate by counting the number of cells attached to the substrate, (*c*) estimating the apoptotic fraction by flow cytometry analyses, and (*d*) observing under microscopy the density of cells attached to the substrate.

Because dimethoxycurcumin is structurally related to curcumin (31), their differential efficiency in antiproliferative and apoptotic activities prompted us to investigate these two compounds for structural characteristics, metabolic profiling after incubation with mouse and human hepatic microsomes, and stability in cultured cells and following dosing in mice. For these studies, we used various mass spectroscopy methodologies. We initially assessed the presence of tautomeric dimethoxycurcumin enol and keto forms, which, like curcumin enol and keto forms, showed distinctly different retention times under gradient conditions in a LC-MS system. Subsequently, the fragmentation behavior of the two compounds was investigated by a hybrid triple-quadrupole linear ion trap LC-MS/MS system, and it was assessed that dimethoxycurcumin exhibited a characteristic fragmentation spectrum. Before proceeding with dimethoxycurcumin metabolic studies, we confirmed previously reported findings (26, 28–30) on the extensive metabolism of curcumin using the described methodology (following incubation with mouse and liver microsomes). We proceeded to identify major metabolites of dimethoxycurcumin following incubation with mouse and human liver microsomes in the presence of NADPH. In comparison with curcumin, metabolism of dimethoxycurcumin was less extensive (metabolites are reported in Table 1). There were limited differences between the metabolites formed in mouse and human microsomes. According to these findings, we propose the dimethoxycurcumin metabolic pathway shown in scheme I (Fig. 4). This is the first report on identification of dimethoxycurcumin metabolites and the putative dimethoxycurcumin metabolic pathway.

A comparative study on the stability of curcumin and dimethoxycurcumin was done with HCT116 cancer cells treated with these two compounds for selected periods and monitoring stability by LC-MS/MS. The relative amount of curcumin was rapidly decreased at 24 h within the cells and was nearly undetectable at 48 h, whereas ~70% of dimethoxycurcumin was detected even at 48 h of incubation with the cells. It is possible that the increased apoptotic activity of dimethoxycurcumin over curcumin, shown in Fig. 1, is associated with the extensive stability of the intact dimethoxycurcumin molecule *in vitro*.

To further characterize dimethoxycurcumin and its ability to play a role as a potential chemotherapeutic agent for cancer, we decided to give dimethoxycurcumin in mice and evaluate its *in vivo* stability. For comparative studies, we included curcumin in the described *in vivo* experiments, a compound with known pharmacokinetic properties and metabolic profile. The results indicated that, following administration (5 mg/kg), both dimethoxycurcumin and curcumin were rapidly cleared from the plasma. However, plasma levels for dimethoxycurcumin were overall higher (~3-fold) in comparison with curcumin, and this stability can in part be explained by the differences in the metabolic profiling data provided in this article. It should be noted that resulting plasma concentrations for both compounds (curcumin and dimethoxycurcumin) were low at 5 mg/kg dose (<1.1 μmol/L for all time points), leading us to the assumption that higher doses and/or different routes of administration would have to be considered to achieve efficacy

with any of the two compounds. Such studies are under way in our laboratory.

In conclusion, both studies, *in vitro* and *in vivo*, seem to support the hypothesis that the differential apoptotic activities of dimethoxycurcumin and curcumin are positively associated with the extent of stability of these two compounds. However, this hypothesis does not exclude the possibility that a dimethoxycurcumin metabolite, not present in the curcumin metabolites, is also associated with or contributes to the increased apoptosis-induced ability. Finally, it is also possible that curcumin is a chemopreventive rather than chemotherapeutic agent for cancer, whereas, reversibly, dimethoxycurcumin is primarily a tumor chemotherapeutic rather than chemoprotective agent. However, this hypothesis warrants further studies of dimethoxycurcumin as an agent for cancer chemoprevention and treatment.

References

1. Gafner S, Lee S-K, Guendet M, et al. Biologic evaluation of curcumin and structural derivatives in cancer chemoprevention model systems. Phytochemistry 2004;65:2849–59.
2. Shishodia S, Sethi G, Aggarwal BB. Curcumin: getting back to the roots. Ann N Y Acad Sci 2005;1056:206–17.
3. Sharma RA, Gescher AJ, Steward WP. Curcumin: the story so far. Eur J Cancer 2005;41:1955–68.
4. Aggarwal BB, Shishodia S. Molecular targets of dietary agents for prevention and therapy of cancer. Biochem Pharmacol 2006;71:1397–421.
5. Maheshwari RK, Singh AK, Gaddipati J, Srimal RC. Multiple biological activities of curcumin: a short review. Life Sci 2006;78:2081–7.
6. Sarkat FH, Li Y. Cell signaling pathways altered by natural chemopreventive agents. Mutat Res 2004;555:53–64.
7. Campbell FC, Collett GP. Chemopreventive properties of curcumin. Future Oncol 2005;1:405–14.
8. Mukhopadhyay A, Bueso-Ramos C, Chatterjee D, Pantazis P, Aggarwal BB. Curcumin downregulates cell survival mechanisms in human prostate cancer cell lines. Oncogene 2001;20:7597–609.
9. Martin-Cordero C, Lopez-Lazaro M, Galvez M, Ayuso MJ. Curcumin as a DNA topoisomerase II poison. J Enzyme Inhib Med Chem 2003;18:505–9.
10. Chaudhary LR, Hruska KA. Inhibition of cell survival signal protein kinase B/Akt by curcumin in human prostate cancer cells. J Cell Biochem 2003;89:1–5.
11. Collett GP, Campbell FC. Curcumin induces c-jun N-terminal kinase-dependent apoptosis in HCT116 human colon cancer cells. Carcinogenesis 2004;25:2183–9.
12. Chendil D, Ranga RS, Meigooni D, Sathishkumar S, Ahmed MM. Curcumin confers radiosensitizing effect in prostate cancer cell line PC-3. Oncogene 2004;23:1599–607.
13. Fang J, Lu J, Holmgren A. Thioredoxin reductase is irreversibly modified by curcumin. A novel molecular mechanism for its anticancer activity. J Biol Chem 2005;280:25284–90.
14. Gao X, Deep D, Jiang H, Lin YB, Dulchavsky SA, Gautam SC. Curcumin differentially sensitizes malignant glioma cells to TRAIL/Apo2L-mediated apoptosis through activation of procaspases and release of cytochrome *c* from mitochondria. J Exp Ther Oncol 2005;5:39–48.
15. Lee KW, Kim JH, Lee HJ, Surh YJ. Curcumin inhibits phorbol ester-induced up-regulation of cycloxygenase-2 and matrix metalloproteinase-9 by blocking ERK1/2 phosphorylation and NF-κB transcriptional activity in MCF10A human breast epithelial cells. Antioxid Redox Signal 2005;7:1612–20.
16. Deeb DD, Jiang H, Gao X, Divine G, Dulchavsky SA, Gautam SC. Chemosensitization of hormone-refractory prostate cancer cells by curcumin to TRAIL-induced apoptosis. J Exp Ther Oncol 2005;5:81–91.
17. Yeh CH, Chen TP, Wu YC, Lin YM, Jing-Lin P. Inhibition of NFκB activation with curcumin attenuates plasma inflammatory cytokines surge and cardiomyocytic apoptosis following cardiac ischemia/reperfusion. J Surg Res 2005;125:109–16.
18. Adams BK, Cai J, Armstrong J, et al. EF24, a novel synthetic curcumin analogue, induces apoptosis in cancer cells via a redox-dependent mechanism. Anticancer Drugs 2005;16:263–75.
19. Lo Tempio MM, Veena MS, Steele HL, et al. Curcumin suppresses growth of head and neck squamous cell carcinoma. Clin Cancer Res 2005;11:6994–7002.
20. Aggarwal BB, Kumar A, Bharti AC. Anticancer potential of curcumin: preclinical and clinical studies. Anticancer Res 2003;23:363–98.
21. Furness MS, Robinson TP, Ehlers T, et al. Antiangiogenic agents: studies on fumagillin and curcumin analogs. Curr Pharm Des 2005;11:357–73.
22. Chakrabarty S, Ghosh U, Bhattacharya NP, Bhattacharya RK, Roy M. Inhibition of telomerase activity and induction of apoptosis by curcumin in K-562 cells. Mutat Res 2006;596:81–90.
23. Wang R, Zhang Y, Banerjee S, Li Y, Sarkar FH. Notch-1 down-regulation by curcumin is associated with the inhibition of cell growth and the induction of apoptosis in pancreatic cancer cells. Cancer 2006;106:2503–13.
24. Sung-ai C, Kumari AL, Khar A. Effect of curcumin on normal and tumor cells: role of glutathione and Bcl-2. Mol Cancer Ther 2004;3:1101–8.
25. Cheng AL, Hsu CH, Lin JK, et al. Phase I clinical trial of curcumin, a chemopreventive agent, in patients with high-risk or pre-malignant lesions. Anticancer Res 2001;21:2895–900.
26. Ireson C, Orr S, Jones JL, et al. Characterization of metabolites of the chemopreventive agent curcumin in human and rat hepatocytes and in the rat *in vivo*, and evaluation of their ability to inhibit phorbol ester-induced prostaglandin E_2 production. Cancer Res 2001;61:1058–64.
27. Sharma RA, McLelland HR, Hill KA, et al. Pharmacodynamic and pharmacokinetic study of oral *Curcuma* extract in patients with colorectal cancer. Clin Cancer Res 2001;7:1894–900.
28. Ireson CR, Jones DJL, Orr S, et al. Metabolism of the cancer chemopreventive agent curcumin in human and rat intestine. Cancer Epidemiol Biomarkers Prev 2002;11:97–104.
29. Pan M-H, Huang T-M, Lin J-K. Biotransformation of curcumin through reduction and glucuronidation in mice. Drug Metab Dispos 2000;27:486–94.
30. Asai A, Miyazawa T. Occurrence of orally administered curcuminoid as glucuronide and glucuronide/sulfate conjugates in rat plasma. Life Sci 2000;67:2785–93.
31. Chen W-F, Deng S-L, Zhou B, Yang L, Liu Z-L. Curcumin and its analogues as potent inhibitors of low density lipoprotein oxidation: H-atom abstraction from the phenolic groups and possible involvement of the 4-hydroxy-3-methoxyphenyl groups. Free Radic Biol Med 2006;40:526–35.
32. Skehan P, Storeng R, Scudiero D, et al. New colorimetric cytotoxicity assay for anticancer drug screening. J Natl Cancer Inst 1990;82:1107–14.
33. Pluquet O, North S, Bhoumik A, Dimas K, Ronai Z, Hainaut A. The cryoprotective aminothiol WR1065 activates p53 through a kinase. J Biol Chem 2003;278:11879–87.
34. Pantazis P, Kozielski AJ, Mendoza JT, Early JA, Hinz HR, Giovanella BC. Camptothecin derivatives induce regression of human ovarian carcinomas grown in nude mice and distinguish between non-tumorigenic and tumorigenic cells *in vitro*. Int J Cancer 1993;53:868–71.
35. Pantazis P, Early JA, Mendoza JT, DeJesus AR, Giovanella BC. Cytotoxic efficacy of 9-nitrocamptothecin in the treatment of human malignant melanoma cells *in vitro*. Cancer Res 1994;54:771–6.
36. Pantazis P, Chatterjee D, Han Z, Wyche JH. Differentiation of human malignant melanoma cells that escape apoptosis following treatment with 9-nitrocamptothecin *in vitro*. Neoplasia 2000;1:231–40.
37. Hu X, Balan KV, Ramos-DeSimone N, Wyche JH, Han Z, Pantazis P. Differential susceptibility to 9-nitrocamptothecin (9-NC)-induced apoptosis in clones derived from a human ovarian cancer cell line: possible implications in the treatment of ovarian cancer patients with 9-NC. Anticancer Drugs 2003;14:427–36.
38. Hollingshead M. Intraperitoneal and subcutaneous tumor models for assessing anti-neoplastic agents on rodents. In: Taylor GP, editor. Current protocols in pharmacology. New York: John Wiley & Sons; 2000. p. 5.28.6–5.20.14.
39. Mague JT, Alworth WL, Payton FL. Curcumin and derivatives. Acta Crystallogr C 2004;C60:608–10.
40. Liu A, Lou H, Zhao L, Fan P. Validated LC/MS/MS assay for curcumin and tetrahydrocurcumin in rat plasma and application to pharmacokinetic study of phospholipid complex of curcumin. J Pharm Biomed Anal 2006;40:720–7.
41. Jiang H, Timmermann B, Gang D. Use of liquid chromatography-electrospray ionization tandem mass spectrometry to identify diarylheptanoids in turmeric (*Curcuma longa* L.) rhizome. J Chromatogr A 2006;1111:21–31.
42. Chowdhury H, Walia S, Saxena V. Isolation, characterization, and insect growth inhibitory activity of major turmeric constituents and their derivatives against *Schistocerca gregaria* (Forsk) and *Dysdercus koenigii* (Walk). Pest Manag Sci 2000;56:1086–92.
43. Mauriala T, Chauret N, Oballa R, Nicoll-Griffith DA, Bateman KP. A strategy for identification of drug metabolites from dried blood spots using triple-quadrupole/linear ion trap hybrid mass spectrometry. Rapid Commun Mass Spectrom 2005;19:1984–92.
44. Hopfgartner G, Husser C, Zell M. Rapid screening and characterization of drug metabolites using a new quadrupole-linear ion trap mass spectrometer. Rapid Commun Mass Spectrom 2003;38:138–50.
45. Ohtsu H, Xiao Z, Ishida J, et al. Antitumor agents. 217. Curcumin analogues as novel androgen receptor antagonists with potential as anti-prostate cancer agents. J Med Chem 2002;45:5037–42.

Clinical Cancer Research

Metabolism and Anticancer Activity of the Curcumin Analogue, Dimethoxycurcumin

Constantin Tamvakopoulos, Konstantinos Dimas, Zacharias D. Sofianos, et al.

Clin Cancer Res 2007;13:1269-1277.